Automatic segmentation of the optic radiation using DTI in glaucoma patients

Ahmed El-Rafei & Joachim Hornegger
Chair of Pattern Recognition, Department of Computer Science,
& Erlangen Graduate School in Advanced Optical Technologies (SAOT),
Tobias Engelhorn & Arnd Dörfler
Department of Neuroradiology,
Simone Wärntges & Georg Michelson
Department of Ophthalmology,
Friedrich-Alexander University Erlangen-Nuremberg, Germany

ABSTRACT: An automated segmentation system of the optic radiation using diffusion tensor imaging (DTI) is proposed. The DTI-data is interpolated in the Log-Euclidean framework to avoid the swelling effect and regularized by diffusion filtering. Based on physiological and anatomical information, robust initial estimates of the optic radiation and the midbrain are obtained using thresholding and connectivity analysis. The estimated optic radiation initializes a statistical level set framework. The optic radiation is segmented by evolving the level set function. The segmentation is refined using the relative position between the optic radiation and the midbrain. The system is tested using eighteen DTI-datasets of glaucoma and normal subjects. The segmentation results were compared to the manual segmentation by a medical expert and found to be in agreement with the known anatomy with 83% accuracy. The automation eliminates the necessity of medical experts' intervention to identify the optic radiation and facilitates future glaucoma studies.

1 INTRODUCTION

Glaucoma is the second leading cause of blindness in the world. The damage caused by glaucoma is irreversible. The progression of glaucoma can be delayed significantly if glaucoma is detected in early stages. Therefore, methods for screening, early diagnosis and better understanding of glaucoma and its progression are needed.

Most of the existing eye imaging modalities focus on imaging the eye in general and the retina in particular. Many studies were performed to investigate the correlation between glaucoma and retinal changes such as retinal nerve fiber atrophy, retinal vessels, and optic disk changes (Lee et al. 1998; Hoffmann et al. 2007; Polo et al. 2009). The human visual system does not only consist of the eye but it extends through the optic nerve into the brain till it reaches the visual cortex. Some studies exist for the correlation between glaucoma and parts of the visual system such as the optic nerve (Hui et al. 2007). As a part of the visual system, the optic radiation is a massive fiber bundle of axons carrying visual information from the lateral geniculate body of the thalamus to the visual cortex.

In this work we aim to provide a system for the automatic identification of the optic radiation in normal and glaucoma patients. DTI is used to segment the optic radiation as it is the only imaging modality that allows for the identification of white matter fibers. This is a step towards a better understanding of the changes caused by glaucoma in this part of the human visual system.

In the last two decades, diffusion tensor imaging has received a lot of attention due to its clinical applications. Furthermore, it is the only imaging modality that allows tracking the white matter fibers in-vivo and non-invasively, and it enables the construction of an atlas of white matter fibers in the human brain (Zhou 2004; Zhang et al. 2005; Basser and Jones 2002; Nucifora et al. 2007; Wakana et al. 2004). DTI is calculated from diffusion weighted magnetic resonance imaging (DW-MRI). Diffusion weighted imaging (DWI) is based on weighting the magnetic resonance images by the diffusion of water molecules (Le Bihan et al. 2001).

Many algorithms were proposed for the identification of white matter tracts using DTI. The dominant category is tractography which is based on following the fiber tracts using the principal diffusion direction (Zhang et al. 2005). Connectivity maps were suggested (Yörük et al. 2005) to explore the connectivity in DTI and to overcome tractography drawbacks such as accumulated errors during the tracking process. Connectivity maps have the disadvantage that they do not provide plausible visualization of the results (i.e. fiber tracts). The split and merge technique (Bozkaya and Acar 2007) provides a degree of membership of small tracts belonging to the same fiber but do not describe the complete fiber pathway. Segmentation approaches of DTI are proposed (Wang and Vemuri 2005; Zhukov et al. 2003; Hamarneh and Hradsky 2006) and are more suitable for identifying coherent densely packed bundles of axons as it avoids the drawbacks from both connectivity maps and tractography such as tracking accumulation errors and the need to merge the individual tracts to obtain fiber bundles. Furthermore, it relies on the coherency within the fiber bundle of interest. Therefore, the segmentation approach is adopted in this work. The proposed segmentation system utilizes the complete tensor information in a statistical level set frame work that takes into consideration the Riemannian nature of the tensor space.

Most of the proposed algorithms did not address the problem of algorithm initialization. They rely on medical experts interaction to select the seed points of the desired fiber tracts in tractography algorithms or the initialization of the segmentation engines to include the desired fiber bundle. The proposed segmentation system utilizes the physiological properties of the optic radiation to produce a robust initialization of the proposed segmentation system in both healthy and pathological subjects with glaucoma.

The segmentation system consists of the following steps: First the diffusion tensor and related anisotropy measures are calculated from the diffusion weighted images. The calculated diffusion tensor data is transformed into the Log-Euclidean framework and interpolated as presented in Section 2. In Section 3, DTI-data is regularized to increase the coherency of the optic radiation fiber bundle before obtaining an initial estimate of the optic radiation using thresholding and connectivity analysis. The midbrain is initially identified using a similar analysis to that of the optic radiation. The system extends the statistical level set framework for DTI segmentation developed by Lenglet et al. (2006) to be used in conjunction with the Log-Euclidean dissimilarity distance as detailed in Section 4. The optic radiation is obtained by iteratively evolving the level set function. Finally, the output from the level set framework is adjusted based on the relative location of the optic radiation and the midbrain. Section 5 contains the experimental results. The conclusion and future work are stated in Section 6.

2 LOG-EUCLIDEAN FRAMEWORK AND DTI INTERPOLATION

The diffusion tensors are 3 x 3 symmetric positive semi-definite matrices that do not form a vector space. The Log-Euclidean framework proposed by Arsigny et al. (2006) provides a Riemannian framework to deal with the diffusion tensors. Using this framework, diffusion tensor space of positive semi-definite matrices can be transformed into the space of symmetric matrices, i.e. a vector space. Moreover, all operations performed on vectors can be used on the vector form of the diffusion tensor in the Log-Euclidean framework.

The Log-Euclidean distance $d_{T_{LE}}$ between tensors T_1 and T_2 is defined by

$$d_{T_{LE}}\left(T_1, T_2\right) = \parallel \log\left(T_1\right) - \log\left(T_2\right) \parallel \qquad (1)$$

where $\log$ is the matrix logarithm.

The interpolation of the DTI-data is necessary in order to obtain a volumetric identification of the optic radiation. Interpolation of diffusion tensors in the Euclidean framework results in the non-physical swelling effect where the average of diffusion tensors with the same determinant has a larger determinant (Corouge et al. 2006). Interpolation in the Log-Euclidean framework avoids the swelling effect at a computationally attractive cost. The diffusion tensor T is interpolated trilinearly at non-grid position x as the Log-Euclidean weighted sum of N tensors in a neighborhood of the non-grid position. The weights are inversely proportional to the spatial distance between the non-grid position and the locations of the tensors in the neighborhood.

3 INITIAL ESTIMATION OF THE OPTIC RADIATION

In this step, the optic radiation and the midbrain are initially identified. The diffusion tensor data is first regularized by applying Perona-Malik diffusion filtering (Perona and Malik 1990) to the vector form of the tensors componentwise. Regularization is performed to reduce the noise and to increase the coherency inside the fiber bundles while preserving the edges.

The initial estimation of the optic radiation is based on the fact that the main fiber bundle of the optic radiation is dominated by diffusion in the anterior-posterior direction. The image is thresholded and binarized on a voxel by voxel basis. The eigenvector of the tensor corresponding to the largest eigenvalue is taken as the principal diffusion direction and the principal diffusion components in the three coordinate axis are compared. The foreground voxels are selected to have an anterior-posterior component greater than a variably selected factor of the sum of the other two components and a fractional anisotropy value greater than 0.15. The remaining voxels that do not satisfy the selection criteria are set as the background of the binary image. A three dimensional connectivity analysis is performed on the binarized image where two voxels are considered connected if they have a common face. Connected objects are determined and the optic radiation is initially identified as the largest object dominated by diffusion in the anterior-posterior direction. This estimation will be used in the segmentation step as an initialization to the used level set framework.

The analysis applied to estimate the optic radiation is similarly applied to identify the midbrain. The analysis takes into account that the midbrain is characterized by diffusion in the superior-inferior direction and is located in the neighborhood of the centers of the axial brain slices. The relative position of the estimated midbrain to the optic radiation will be used in a later step to refine the segmentation of the optic radiation.

4 SEGMENTATION USING STATISTICAL LEVEL SET FRAMEWORK

The segmentation is performed in two steps. First, the DTI is segmented using a statistical level set framework. The initially estimated optic radiation is used as the initial surface. Second, the results from the level set framework are adjusted based on anatomical information between the midbrain and the optic radiation.

We extend the surface evolution framework developed by Lenglet et al. (2006) to work with the Log-Euclidean dissimilarity measure given in equation 1. In the following we present briefly the mathematical formulation of the level set framework in the case of the Log-Euclidean framework. For further details see (Lenglet et al. 2006; Arsigny et al. 2006). The diffusion tensor $T(x)$ at voxel x is mapped to the space of symmetric matrices and transformed into a vector form $\beta(x)$ using the following mapping:

$$\beta(x) = vec\left(\log\left(T(x)\right)\right) \tag{2}$$

where vec is the mapping of the 3 x 3 symmetric matrices to the corresponding 6-dimensional vectors.

Using the notation in equation 2, the mean, covariance matrix and Gaussian distribution between diffusion tensors can be defined as :

$$\mu_{LE} = \frac{1}{N}\sum_{i=1}^{N}\beta\left(x_i\right) \tag{3}$$

$$Cov_{LE} = \frac{1}{N-1}\sum_{i=1}^{N}\left(\beta\left(x_i\right)-\mu_{LE}\right)\left(\beta\left(x_i\right)-\mu_{LE}\right)^T \tag{4}$$

$$\begin{aligned} P_{LE}\left(\beta\left(x_i\right)\right) &= \frac{1}{\sqrt{(2\pi)^6|Cov_{LE}|}} \\ &\exp\left(-\frac{\left(\beta\left(x_i\right)-\mu_{LE}\right)^T Cov_{LE}^{-1}\left(\beta\left(x_i\right)-\mu_{LE}\right)}{2}\right) \end{aligned} \tag{5}$$

The spatial gradient of the diffusion tensor in the vector space is given by

$$\begin{aligned} |\nabla\beta(x)|^2 = \frac{1}{2}\sum_{k=1}^{3}\sum_{s=\pm1} tr\Big(&\left(\beta(x)-\beta(x+se_k)\right) \\ &\cdot\left(\beta(x)-\beta(x+se_k)\right)^T\Big) \end{aligned} \tag{6}$$

where the e_k, k=1, 2 ,3 denotes the canonical basis of $\mathbb{R}_3$. $s \in \{1,-1\}$ and denotes the forward and backward approximations of the gradient. tr is the trace of a matrix.

The idea of the statistical surface evolution is to seek the optimal partitioning of the tensor image (β in the Log-Euclidean case) by maximizing a posteriori frame partition probability for the diffusion tensor image with image domain Γ. This is done in a level set framework, where the image is partitioned into three regions based on a level set function ϕ: inside Γ_{in}, outside Γ_{out} or on the boundary Γ_B. The boundary is defined as the zero-crossing of ϕ. The probability distributions of the inside p_{in} and outside p_{out} regions are modeled by Gaussian distributions on tensors using equation 5. The partition probability is given by

$$\begin{aligned} P(\beta|\phi) = &\prod_{x\in\Gamma_{in}} p_{in}(\beta(x)) \\ &\cdot\prod_{x\in\Gamma_{out}} p_{out}(\beta(x)) \prod_{x\in\Gamma_B} p_b(\beta(x)) \end{aligned} \tag{7}$$

The boundary probability distribution p_b is selected to have a value of approximately one for high gradients of the diffusion tensors (using equation 6 for gradient calculations) and a value of approximately zero for low gradients as the following relation indicates.

$$p_b\left(\beta\left(x\right)\right) \propto \exp\left(-g\left(\left|\nabla\beta\left(x\right)\right|\right)\right) \tag{8}$$

where $g(u) = 1/(1+u^2)$.

This leads to the energy minimization formulation:

$$\begin{aligned} &E(\phi, \mu_{LE_{in/out}}, Cov_{LE_{in/out}}) \\ &= \nu\int_{\Gamma}\delta(\phi)|\nabla\phi|dx + \int_{\Gamma}\delta(\phi)|\nabla\phi|g(|\nabla\beta\left(x\right)|)dx \\ &- \int_{\Gamma_{in}}\log(p_{in}(x))dx - \int_{\Gamma_{out}}\log(p_{out}(x))dx \end{aligned} \tag{9}$$

with the corresponding Euler-Lagrange equation

$$\begin{aligned} \frac{\partial\phi}{\partial t} = \delta(\phi)\Bigg(&\left(\nu + g(|\nabla\beta\left(x\right)|)\right) div\left(\frac{\nabla\phi}{|\nabla\phi|}\right) \\ &+\frac{\nabla\phi}{|\nabla\phi|}\cdot\nabla g(|\nabla\beta\left(x\right)|) + \log\left(\frac{p_{in}}{p_{out}}\right)\Bigg) \end{aligned} \tag{10}$$

The level set function in equation 10 is evolved iteratively to obtain the desired segmentation. The output from the level set framework contains the fiber bundle of the optic radiation and additional bundles connected to it such as the optic tract. The segmented region is automatically adjusted in order to confine the segmentation results to the part representing the optic radiation based on its relative position to the segmented midbrain. A plane is automatically selected corresponding to the anterior boundary of the segmented midbrain. The segmentation results anterior to the selected plane are eliminated.

5 EXPERIMENTAL RESULTS

Eighteen subjects were examined by ophthalmologists and categorized into two age matched groups. The first group represents the subjects that were diagnosed with primary open angle glaucoma and the other group represents the normal subjects. The glaucoma group contains 9 subjects with a mean$\pm$standard deviation age of (66$\pm$11.8 years) with 7 females and 2 males, while the normal group contains 9 subjects with a mean$\pm$standard deviation age of (67.1$\pm$8.1 years) with 6 females and 3 males. Further ophthalmological and neuroradiological examinations were performed and did not provide indications of microangiopathy or irregularly developed optic radiation.

The subjects were scanned using a 3T-MRI scanner. The diffusion weighted images were acquired using a single-shot, spin echo, echo planar imaging (EPI) as an imaging sequence with repetition time (TR) 3400 ms, echo time (TE) = 93 ms, field of view (FoV) 230 x 230 mm^2, acquisition matrix size of 128 x 128 reconstructed to 256 x 256, seven signal averages, and partial Fourier acquisition = 60%. The axial slices have a thickness of 5 mm and 1 mm interslice spacing. Diffusion weighting with a maximal b-factor of 1000 s/mm^2 along 15 icosahedral directions complemented by one scan with b = 0. The diffusion tensors were calculated from the measured diffusion weighted images along with fractional anisotropy, eigenvectors and eigenvalues on a voxel by voxel basis.

The segmentation system is applied to the DTI-datasets and the optic radiation in the two groups is identified. The left side of Figure 1 shows the final segmented optic radiation on non-diffusion weighted axial slices with b = 0 from three sample subjects (two normal and one with glaucoma). The color coded fractional anisotropy representation of the DTI-data is demonstrated on the right side of the figure.

The segmentation results were evaluated by comparing them with a manual segmentation of the optic radiation main fiber bundle performed by a medical expert. The accuracy of the segmentation system is calculated as the percentage of the overlap volume between the automatic segmentation results and the manual segmentation to the total volume of the manually segmented optic radiation. The accuracy of the segmentation results is 83% for both the normal and the glaucoma groups.

The analysis of the segmentation errors showed that most of the errors are in the region where the optic radiation branches in the proximity of the visual cortex as indicated by arrows in Figure 1. Due to the branching of the optic radiation in this region, the incoherency increases and the anterior-posterior direction is no longer the dominating diffusion direction which is the principal segmentation assumption for the proposed algorithm. The algorithm is robust and produces comparable segmentation accuracy in both groups in spite of the atrophy of the optic radiation in case of glaucoma patients accompanied with increased incoherency. This robustness is due to the dependence of the system on the physiological and anatomical properties which are slightly affected by glaucoma.

6 CONCLUSION AND FUTURE WORK

A system has been proposed for the automatic segmentation of the optic radiation using DTI based on dissimilarity measure and the coherency property within the optic radiation fiber bundles. The automation eliminates medical-experts' intervention for identifying the optic radiation and allows the processing of large number of subjects. The system initialization problem is addressed by utilizing prior knowledge about the physiological and anatomical properties of the optic radiation to automatically provide robust estimation of the optic radiation. The incorporation of the Log-Euclidean framework in the statistical level set framework is suitable and efficient for DTI segmentation because it accounts for the Riemannian nature of the tensor space and incorporates the whole tensor information in a probabilistic framework. The system is implemented and tested using real DTI-data. The experimental results indicate that the system shows high efficiency in determining the main fiber bundle of the optic radiation for normal subjects as well as pathological subjects with glaucoma.

The automated identification of the optic radiation will be utilized in a following study to investigate the correlation between glaucoma and the quantification of the changes occurred in the optic radiation. This aims to give further insight into the glaucoma disease and its effect on the various parts of the human visual system. Future work is the identification of the optic radiation connectivity on the visual cortex. This requires the development of a robust tractography algorithm to be able to accurately identify the highly

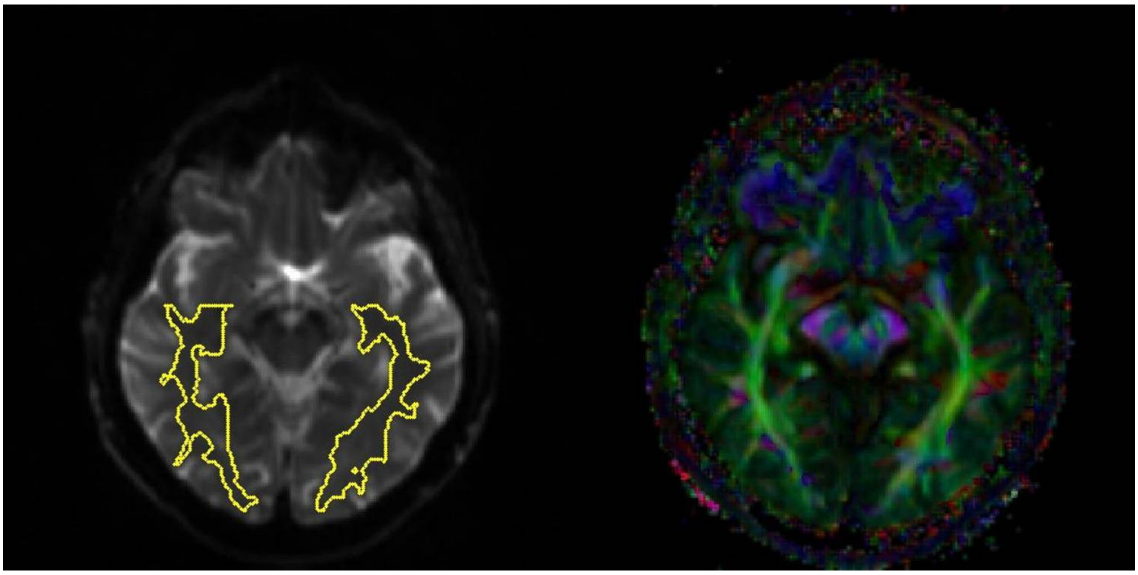

(a)

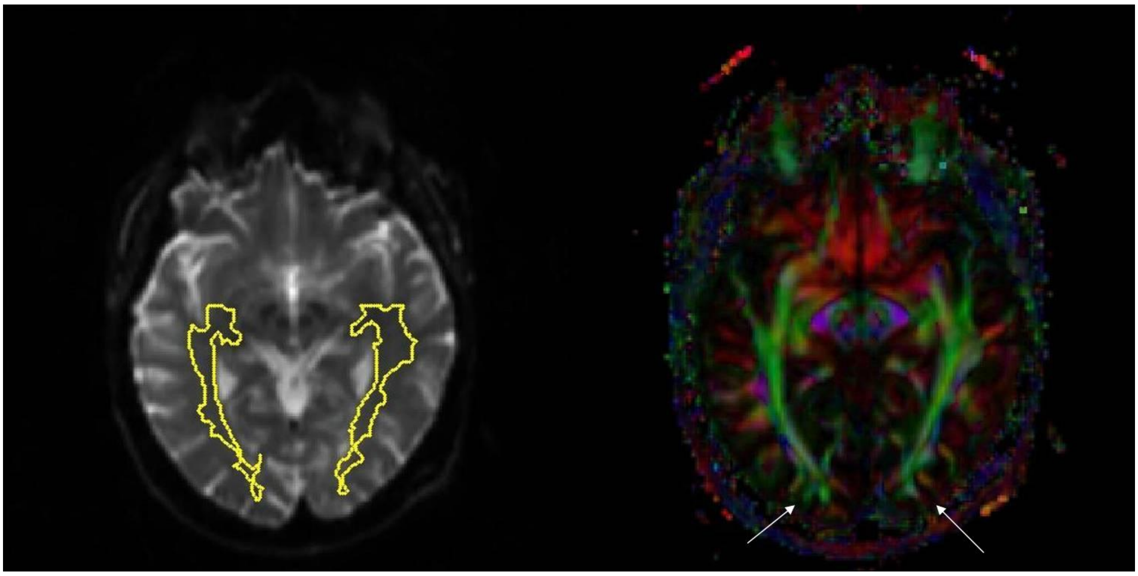

(b)

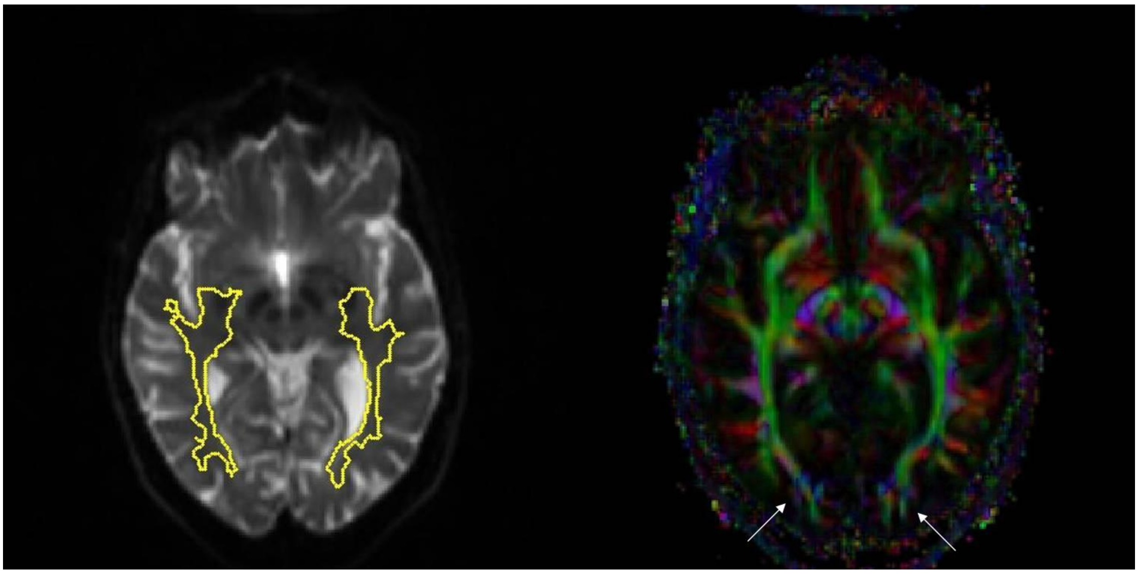

(c)

Figure 1. Segmentation of the optic radiation in three sample subjects : (a,b) normal subjects, (c) subject with glaucoma. The main fiber bundle of the optic radiation and the lateral geniculate nucleus (LGN) of the visual pathway are clearly identified. The arrows indicate the region where the optic radiation branches and the incoherency within the bundle increases

variable branches of the optic radiation while taking into consideration the complex fiber situations (e.g. crossing, branching, etc…) and the uncertainties in the diffusion tensor data.

7 ACKNOWLEDGMENTS

The authors would like to thank Dr. B. Acar from Bogazici University (www.vavlab.ee.boun.edu.tr) for the valuable discussion of the segmentation system. The authors gratefully acknowledge funding of German academic exchange service (DAAD) and the Erlangen Graduate School in Advanced Optical Technologies (SAOT) by the German National Science Foundation (DFG) in the framework of the excellence initiative.

REFERENCES

Arsigny, V., P. Fillard, X. Pennec, and N. Ayache (2006). Log-Euclidean metrics for fast and simple calculus on diffusion tensors. *Magnetic Resonance in Medicine 56*(2), 411–421.

Basser, P. J. and D. K. Jones (2002). Diffusion-tensor MRI: theory, experimental design and data analysis - a technical review. *NMR Biomed 15*(7-8), 456–467.

Bozkaya, U. and B. Acar (2007). SMT: Split and merge tractography for DT-MRI. In *MICCAI, Brisbane, Australia. Lecture Notes in Computer Science*, Volume 4792, pp. 153–160. Springer.

Corouge, I., P. Fletcher, S. Joshi, S. Gouttard, and G. Gerig (2006). Fiber tract-oriented statistics for quantitative diffusion tensor MRI analysis. *Medical image analysis 10*(5), 786–798.

Hamarneh, G. and J. Hradsky (2006). DTMRI segmentation using DT-snakes and DT-livewire. In *IEEE International Symposium on Signal Processing and Information Technology*, pp. 513–518.

Hoffmann, E., L. Zangwill, J. Crowston, and R. Weinreb (2007). Optic disk size and glaucoma. *Survey of Ophthalmology 52*(5), 32–49.

Hui, E., Q. Fu, K. So, and E. Wu (2007). Diffusion tensor MR study of optic nerve degeneration in glaucoma. In *Engineering in Medicine and Biology Society, 2007. EMBS 2007. 29th Annual International Conference of the IEEE*, pp. 4312–4315.

Le Bihan, D., J. Mangin, C. Poupon, C. Clark, S. Pappata, N. Molko, and H. Chabriat (2001). Diffusion tensor imaging: concepts and applications. *Journal of Magnetic Resonance Imaging 13*(4), 534–546.

Lee, S., K. Uhm, and C. Hong (1998). Retinal vessel diameter in normal and primary open-angle glaucoma. *Korean Journal of Ophthalmology: KJO 12*(1), 51–59.

Lenglet, C., M. Rousson, and R. Deriche (2006). DTI segmentation by statistical surface evolution. *IEEE Transactions on Medical Imaging 25*(6), 685–700.

Nucifora, P., R. Verma, S. Lee, and E. Melhem (2007). Diffusion-tensor MR imaging and tractography: exploring brain microstructure and connectivity. *Radiology 245*(2), 367–384.

Perona, P. and J. Malik (1990). Scale-space and edge detection using anisotropic diffusion. *IEEE Transactions on Pattern Analysis and Machine Intelligence 12*(7), 629–639.

Polo, V., J. Larrosa, A. Ferreras, F. Mayoral, V. Pueyo, and F. Honrubia (2009). Retinal nerve fiber layer evaluation in open-angle glaucoma. *Ophthalmologica 223*(1), 2–6.

Wakana, S., H. Jiang, L. Nagae-Poetscher, P. van Zijl, and S. Mori (2004). Fiber tract-based atlas of human white matter anatomy. *Radiology 230*(1), 77–87.

Wang, Z. and B. Vemuri (2005). DTI segmentation using an information theoretic tensor dissimilarity measure. *IEEE Transactions on Medical Imaging 24*(10), 1267–1277.

Yörük, E., B. Acar, and R. Bammer (2005). A physical model for MR-DTI based connectivity map computation. In *MICCAI, Palm Springs, CA. Lecture Notes in Computer Science*, Volume 3749, pp. 213–220. Springer.

Zhang, J., H. Kang, and N. Cao (2005). Fiber tractography in diffusion tensor magnetic resonance imaging: a survey and beyond. Technical Report 437/05, Department of Computer Science, University of Kentucky.

Zhou, X. (2004). Diffusion tensor imaging: techniques and clinical applications. *Engineering in Medicine and Biology Society, 2004. IEMBS '04. 26th Annual International Conference of the IEEE 2*, 5223–5225.

Zhukov, L., K. Museth, D. Breen, R. Whitaker, and A. Barr (2003). Level set modeling and segmentation of DT-MRI brain data. *Journal of Electronic Imaging 12*(1), 125–133.